USC–SIPI REPORT #339

Ultra-Wide Bandwidth Signal Propagation for Indoor Wireless Communications

by

Moe Z. Win and Robert A. Scholtz

June 1997

Signal and Image Processing Institute
UNIVERSITY OF SOUTHERN CALIFORNIA
Department of Electrical Engineering-Systems
3740 McClintock Avenue, Room 400
Los Angeles, CA 90089-2564 U.S.A.

Ultra-Wide Bandwidth Signal Propagation for Indoor Wireless Communications

Moe Z. Win and Robert A. Scholtz
Communication Sciences Institute
Department of Electrical Engineering-Systems
University of Southern California, Los Angeles, CA 90089-2565 USA

Mark A. Barnes
Time Domain Systems, Inc.
6700 Odyssey Drive, Suite 100, Huntsville, AL 35806 USA

Abstract— **An ultra-wide bandwidth (UWB) signal propagation experiment is performed in a typical modern office building in order to characterize the UWB signal propagation channel. The bandwidth of the signal used in this experiment is in excess of one GHz. Robustness of the UWB signal to fades is quantified through histograms and cumulative distributions of the signal quality in various locations of the building. The results show that UWB signal does not suffer fades.**

I. Introduction

PROPAGATION environments place fundamental limitations on the performance of wireless communications systems. The existence of multiple propagation paths (multipath), with different time delays, gives rise to complex, time-varying transmission channels. A line-of-site path between the transmitter and receiver seldom exists in indoor environments, because of natural or man-made blocking, and one must rely on the signal arriving via multipath.

Many propagation measurements have been made over the years on both indoor and outdoor channels with much "narrower bandwidths" [1]–[18]. A comprehensive reference on the indoor propagation channels (a total of 281 references) can be found in the tutorial survey paper by Hashemi [9]. Some of the work by Rappaport [1]–[5] and a few other papers [6]–[8] are listed here as selected references. Although the research described in this paper does not cover outdoor propagation channels, the classic works on outdoor propagation channels by Turin [10], [11], by Cox [14]-[17], and by Nielson [18] are noted here for their excellent measurement procedures and data reduction techniques. However, these measurements are inadequate for ultra-wide bandwidth (UWB) transmission systems, and characterization of UWB signal propagation channels has not been available previously in the literature. Careful characterization the UWB signal propagation channel is prudent for determining optimum methods, in order to achieve the quality communication.

The research described in this paper was supported in part by the Joint Services Electronics Program under contract F49620-94-0022, and in part by the Integrated Media Systems Center, a National Science Foundation Engineering Research Center with additional support from the Annenberg Center for Communication at the University of Southern California and the California Trade and Commerce Agency.

The corresponding author can be reached by E-mail at win@milly.usc.edu

II. Experimental Design and Measurement Apparatus

A short duration pulse, with sub-nanosecond duration, is used to probe the propagation channel. The received signal represents the convolution between the excitation pulse and the impulse response of the channel. The time varying characteristic of the channel can be observed by periodic repetition of the pulse transmission. The duration of the single pulse, inversely proportional to the bandwidth of the transmission, determines the *multipath resolution*, i.e., the minimum discernible path between individual multipath components. The period of the periodic pulse signal transmission determines the maximum measurable multipath delay. Hence, successive multipath components with differential delay greater than the width of the pulse and within one period of the periodic pulse transmission can be measured unambiguously.

A block diagram of the measurement apparatus is shown in Fig. 2. The transmitter consists of a periodic pulse generator that transmits pulses every 500 nanoseconds using a step recovery diode-based pulser connected to a UWB antenna. The receiver consists of a receiving antenna, a trigger probing antenna, a wideband low noise amplifier (LNA), and a digital sampling oscilloscope (DSO). Multipath profiles are captured by the DSO and sent over a HPIB bus to a personal computer for storage. A probe antenna, in proximity to the transmitting antenna, supplies a trigger signal to the DSO by a long fixed length coaxial cable. Therefore, all recorded multipath profiles have the same absolute delay reference, and time delay measurements of the signals arriving to the receiving antenna via different propagation paths can be made. During each of the multipath profile measurement, both the transmitter and receiver were kept stationary. The multipath propagation channel was frozen during the measurement time by ensuring that people in the vicinity of the transmitting and receiving antenna were not moving.

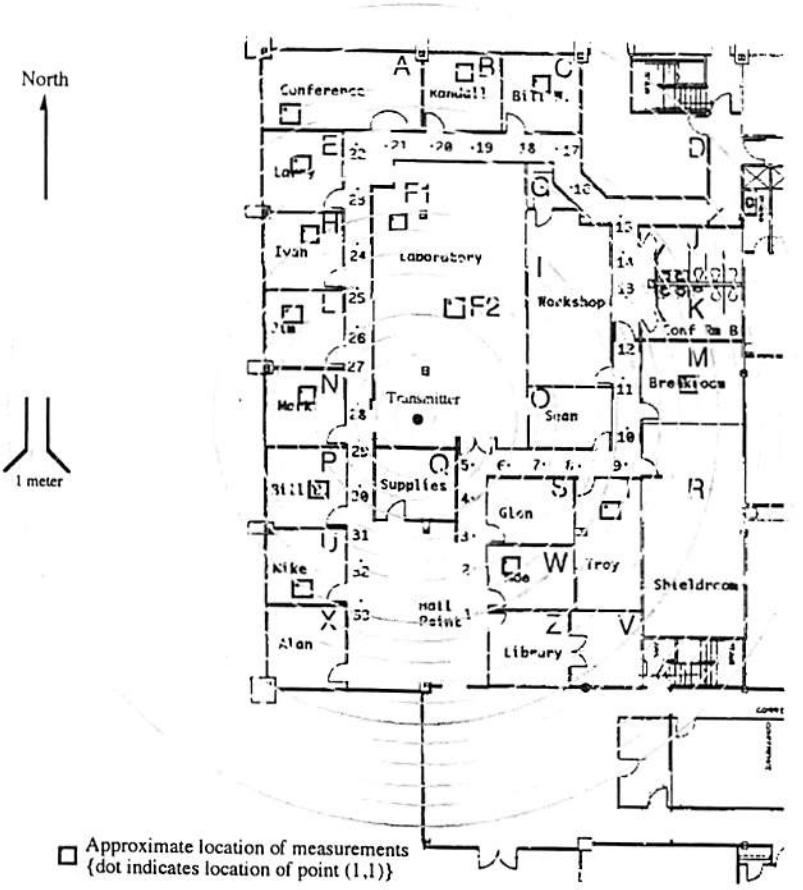

Fig. 1. The floor plan of a typical modern office building where the propagation measurement experiment was performed. The concentric circles are centered on the transmitting antenna and are a spaced at 1 meter intervals.

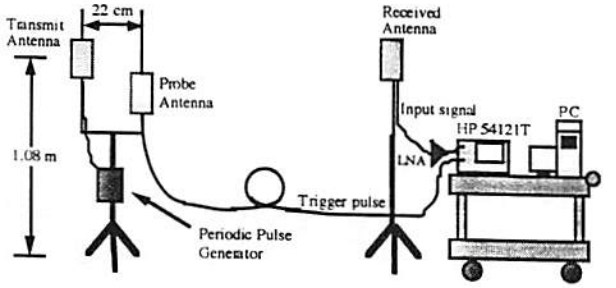

Fig. 2. A block diagram of the measurement apparatus.

III. Results

Figure 1 shows the floor plan of the modern office building where the propagation measurement experiment was performed. Each of the rooms is labeled alphanumerically. Walls around offices are framed with metal studs and covered with plaster board. The wall around the laboratory is made from acoustically silenced heavy cement block. There are steel core support pillars throughout the building, notably along the outside wall and two within the laboratory itself. The shield room's walls and door are metallic. The transmitter is kept stationary in the central location of the building near a computer server in a laboratory denoted by F. The transmitting antenna is located 165 cm from the floor and 105 cm from the ceiling. Figure 3 shows the transmitted pulses measured by the receiving antenna, located 1 m away from the transmitting antenna with the same height. Measurements were made while the vertically polarized receiving antenna was rotated about its axis in 45° steps. Measurements shown in Fig. 3 are labeled 0°, 45°, and 90°, where 0° refers to the case where the transmitting and receiving antennas are facing each other. Figure 3 illustrates that the radiation pattern of the antenna used in the experiment is circularly symmetric around the vertical axis. Notice from the building layout diagram given in Fig. 1 that the closest object to the measurement apparatus is the south wall of laboratory F, which is at least 1 meter away. The signal arriving to the receiving antenna, except the line-of-sight (LOS) signal, must travel a minimum distance of 3 meters. The initial multipaths come form floor and ceiling, 5.2 nanoseconds and 4.1 nanoseconds after the LOS signal respectively, and hence the first 10 nanoseconds of the recorded waveforms in Fig. 3 represent clean pulse arriving via the direct LOS path and not corrupted by multipath components.

Multipath profiles were measured at various locations in the rooms and hallways throughout the building. Specifically, data was collected at 14 different rooms and hallways. In each room, 300 nanoseconds wide windows of multipath measurements were made at 49 different locations over a 3

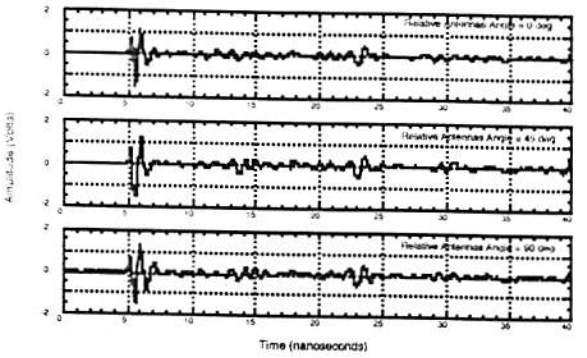

Fig. 3. Transmitted pulses measured by the receiving antenna located 1 m away from the transmitting antenna with the same height. Measurements were made while the vertically polarized receiving antenna was rotated about its axis, where 0° refers to the case in which the transmitting and the receiving antenna are facing at each other.

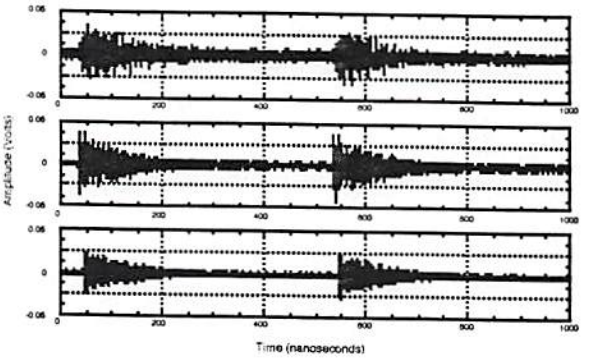

Fig. 4. Average multipath measurements of 32 sequentially measured multipath profiles where the receiver is located at the same exact locations in offices U, W and M. The measurement grids are 10, 8.5, and 13.5 meters away from the transmitter respectively.

feet by 3 feet grid. The approximate location of these measurement grids in each room are shown in Fig. 1. They are arranged spatially in a 7x7 square grid with 6 inch spacing. Each location on the grid is numbered as (i, j), where i represents the rows and j represents the column of the grid. As a convention, the top row is always parallel and adjacent to the north wall of the room. The receiving antenna is located 120 cm from the floor and 150 cm from the ceiling. This antenna height is envisioned to be typical for future indoor applications.

A single multipath profile of 1000 nanoseconds long, which captures the response of two successive probing pulses, was also made in each room. Figure 4 shows the 1000 nanoseconds long measurement, where two back to back multipath measurement cycles are captured by the receiver located in offices U, W and M respectively. The approximate distances between the transmitter and the location of these measurement grids located in offices U, W and M are 10, 8.5, and 13.5 meters respectively. Figure 4 also shows that the response of the first probing pulse has decayed (is sufficiently settled down) before the next pulse arrives at the antenna. Substantial differences in the noise floor at various locations throughout the building is observed. Specifically, the multipath profiles recorded in the offices W and M have a substantially lower noise floor compared to the profiles recorded in office U. This can be explained, with the help of the floor plan given in Fig. 1, by observing: Office U is situated at the edge of the building with large glass window. Offices W and M are situated roughly in the middle of the building. Furthermore, offices W and M are adjacent to room R which is shielded from electromagnetic radiation. Interference from radio stations, television stations, cellular and paging towers, and other external electromagnetic interference (EMI) sources are attenuated by the shielded walls and multiple layers of other regular walls. The increased noise floor is generally observed for all the measurements made in offices located at edges of the building with large glass windows.

Figure 5 shows the averaged multipath profiles measured in office P at locations (4,1), (4,4) and (4,7) along the horizontal cross section of the grid with three different aligned positions of one foot apart. The distance between the receiver in the office P and the transmitter is approximately 6 meters, relatively close compared to other rooms. The data that is collected in this room represents typical UWB signal transmissions for the "high SNR" case. Notice that the direct path response (leading edge of the responses) suggests that the location of the receiver for the lower trace is closer to the transmitter than that of the upper trace. This fact can be verified easily by the floor plan given in Fig. 1. Multipath delay spreads on the order of a hundred nanoseconds were observed.

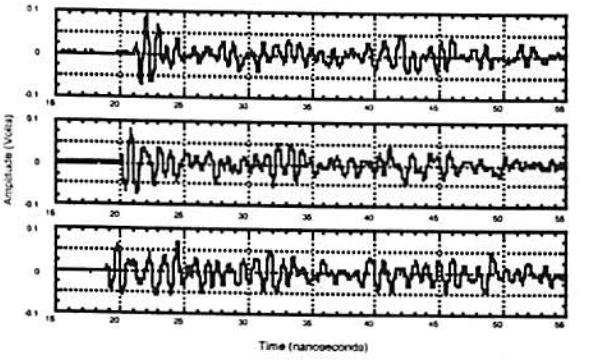

Fig. 5. Averaged multipath profiles of 40 nanoseconds window measured in office P, along the horizontal cross section of the grid at three different aligned positions of one foot apart. The transmitter is approximately 6 meters from the receiver representing typical UWB signal transmissions for the "high SNR" case.

To understand the effect of office doors, two multipath profiles were recorded at the same location in office B. One profile was recorded with the office door open and the other profile was recorded with the office door closed. No noticeable difference between these two measurements was observed. The effect of the large computer monitor was also considered. The receiving antenna was placed near a

large computer monitor in office C and measurements were made. A slight increase in noise floor was observed when the computer monitor was turned on.

IV. Robustness of the UWB Signal to Fades

Robustness of the UWB signal to fades can be assessed by measuring the received energy in various locations of the building relative to the received energy at a reference point. Mathematically, the *signal quality* at a location (i, j) can be defined as

$$Q_{i,j} = 10\log_{10} E_{i,j} - 10\log_{10} E_{\text{ref}} \quad [\text{dB}]. \qquad (1)$$

The received energy $E_{i,j}$ at a location (i, j) is given by

$$E_{i,j} = \int_0^T |r_{i,j}(t)|^2 dt, \qquad (2)$$

where $r_{i,j}(t)$ is the measured multipath at location (i, j) and T is the observation time. The reference energy E_{ref} is chosen to be the energy in the LOS path measured by the receiver located 1 meter away from the transmitter.

The signal quality $Q_{i,j}$ is calculated for the measurements made at 741 different locations (14 different rooms with 49 locations/room, 21 locations in the shield room, and 34 locations around the hallways). First and second order local statistics of the signal quality are calculated. That is, the mean and variance of the signal quality based on 49 spatial sample points (except 21 spatial points for room R, and 34 spatial points for hallways) in each room are estimated by

$$\hat{\mu} = \frac{1}{N}\sum_{i,j} Q_{i,j}, \qquad (3)$$

and

$$\hat{\sigma}^2 = \frac{1}{N-1}\sum_{i,j}(Q_{i,j} - \hat{\mu})^2. \qquad (4)$$

It can be shown that these estimate are a function of complete sufficient statistics if the received signal energy $E_{i,j}$ are random samples from normal families. Then by the Lehmann-Scheffé theorem [19], the estimates given by (3) and (4) are unique and gives the uniformly minimum variance unbiased estimates.

Table I shows the estimates of the mean and the variance of the signal quality in each room based on 49 sample (except 21 samples for room R, and 34 samples for hallways). The histograms and the cumulative distribution functions of the signal quality based on 49 spatial local sample points in each room (except 21 samples for room R, and 34 samples for hallways) are shown in Fig. 6 and Fig. 7 respectively. These figures along with Table I indicates that the signal energy per received multipath waveform varies by at most 5 dB as receiving position varies over the measurement grid within a room. This clearly demonstrates the robustness of UWB signal transmissions in a severe fading environments, and that UWB radio have the potential for fade-free communications even in this severe indoor multipath environment. In some situations, the transmitted power potentially can be reduced by 10-30 dB, since only a *small fading margin* in communication link budget is required to guarantee the reliable communication of an UWB radio.

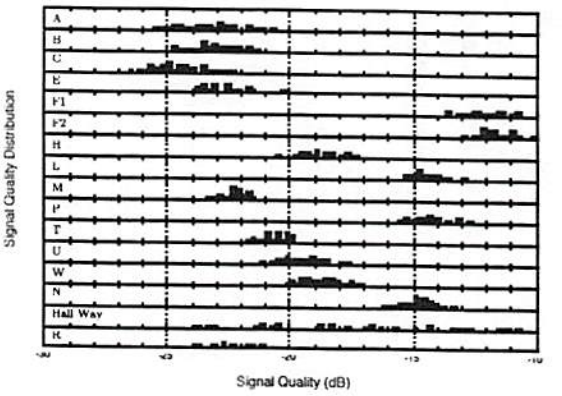

Fig. 6. The histograms of the signal quality based on 49 spatial sample points (except 21 spatial points for room R, and 34 spatial points for hallways) in each room. Total of 741 measurements were used in this plot.

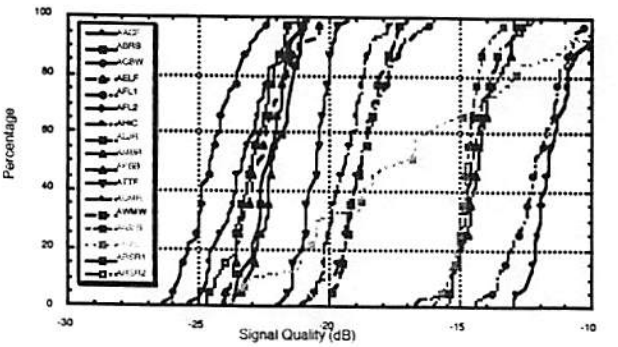

Fig. 7. The cumulative distribution functions of the signal quality based on 49 spatial sample points (except 21 spatial points for room R, and 34 spatial points for hallways) in each room. Total of 741 measurements were used in this plot.

V. Conclusions

Extensive UWB propagation measurements were made in 14 different rooms and hallways of a modern office building using a periodic pulse generator that transmits UWB pulses every 500 nanoseconds. Multipath measurements of 300 nanoseconds long window were made at 49 different locations arranged spatially in a 7x7 square grid with 6 inch spacing covering 3 feet by 3 feet. The same absolute delay reference for all recorded multipath profiles was achieved, and the time delay measurements of the signals arriving to the receiving antenna via different propagation paths were made.

Increased noise floor was generally observed for all the measurements made in offices located at edges of the building with large glass windows; and is attributed to radio sta-

TABLE I
SIGNAL QUALITY STATISTICS

Office	≈ distance (meters)	Minimum (dB)	Maximum (dB)	$\hat{\mu}$ (dB)	Median (dB)	$\hat{\sigma}$ (dB)	# of Samples
F2	5.5	-12.9970	-9.64586	-11.5241	-11.6813	0.8161	49
N	5.5	-16.0060	-13.2949	-14.7260	-14.7690	0.5892	49
P	6.0	-15.5253	-12.2185	-14.2373	-14.2820	0.8091	49
L	8.0	-16.6966	-12.4310	-14.4500	-14.5538	0.8342	49
W	8.5	-20.0157	-17.0351	-18.7358	-18.7425	0.7622	49
F1	9.5	-14.4064	-9.79770	-12.0986	-12.1407	1.0563	49
H	10.0	-21.0415	-16.1628	-18.7141	-18.8142	1.1240	49
U	10.0	-21.1719	-17.6232	-19.4275	-19.4092	0.8024	49
T	10.5	-21.9113	-19.2986	-20.6100	-20.5419	0.5960	49
R	10.5	-23.7221	-20.8867	-22.2675	-22.3851	0.8686	21
M	13.5	-23.8258	-20.9277	-22.2568	-22.2064	0.6439	49
E	13.5	-24.1454	-20.2000	-22.5973	-22.7824	1.0332	49
A	16.0	-25.4171	-20.7822	-23.2826	-23.3541	1.1512	49
B	17.0	-24.7191	-21.2006	-22.9837	-22.9987	0.8860	49
C	17.5	-26.4448	-22.3120	-24.4842	-24.5777	1.0028	49
Hallways		-23.8342	-6.72469	-16.9317	-17.3286	4.5289	34

tions, television stations, cellular and paging towers, and other external electromagnetic interference (EMI) sources coexisting in the same bandwidth. The effects of office doors, large computer monitors were investigated and no substantial effects were observed. Robustness of the UWB signal to fades is quantified through histograms and cumulative distributions of the signal quality in various locations of the building. The results show that UWB signal does not suffer fades. Therefore, very little fading margin is required to guarantee the reliable communication.

ACKNOWLEDGMENTS

The authors wish to thank Troy Fuqua, Glenn Wolenec, Ivan Cowie, and Larry Fullerton of Time Domain Systems, and Paul Withington of Pulson Communications for several helpful discussions concerning the technology, capabilities, and signal processing of impulse signals.

REFERENCES

[1] J. B. Andersen, T. S. Rappaport, and S. Yoshida, "Propagation measurements and models for wireless communications channels," *IEEE Commun. Mag.*, vol. 33, pp. 42–49, Jan. 1995.

[2] T. S. Rappaport and C. D. McGillem, "UHF fading in factories," *IEEE J. Select. Areas Commun.*, vol. SAC-7, pp. 40–48, Jan. 1989.

[3] T. S. Rappaport, "Characterization of UHF multipath radio channels in factory buildings," *IEEE Trans. Antennas Propagat.*, vol. AP-37, pp. 1058–1069, Aug. 1989.

[4] T. S. Rappaport, S. Y. Seidel, and K. Takamizawa, "Statistical channel impulse response models for factory an open plan building radio communication system design," *IEEE Trans. Commun.*, vol. COM-39, pp. 794–807, May 1991.

[5] S. Y. Seidel and T. S. Rappaport, "914 MHz path loss prediction models for indoor wireless communications in multifloored buildings," *IEEE Trans. Antennas Propagat.*, vol. AP-40, pp. 207–217, Feb. 1992.

[6] D. M. J. Devasirvatham, "Multipath time delay jitter measured at 850 MHz in the portable radio environment," *IEEE J. Select. Areas Commun.*, vol. SAC-5, pp. 855–861, June 1987.

[7] A. A. Saleh and R. A. Valenzuela, "A statistical model for indoor multipath propagation," *IEEE J. Select. Areas Commun.*, vol. SAC-5, pp. 128–137, Feb. 1987.

[8] R. J. Bultitude, S. A. Mahmoud, and W. A. Sullivan, "A comparison of indoor radio propagation characteristics at 910 MHz and 1.75 GHz," *IEEE J. Select. Areas Commun.*, vol. SAC-7, pp. 20–30, Jan. 1989.

[9] H. Hashemi, "The indoor radio propagation channel," *Proc. IEEE*, vol. 81, pp. 943–968, July 1993.

[10] G. Turin, F. D. Clapp, T. L. Johnston, S. B. Fine, and D. Lavry, "A statistical model of urban multipath propagation," *IEEE Trans. on Vehicul. Technol.*, vol. VT-21, pp. 1–9, Feb. 1972.

[11] G. Turin, "Introduction to spread-spectrum antimultipath techniques and their application to urban digital radio," *Proc. IEEE*, vol. 68, pp. 328–353, Mar. 1980.

[12] H. Suzuki, "A statistical model for urban radio propagation," *IEEE Trans. Commun.*, vol. 25, pp. 673–680, July 1977.

[13] H. Hashemi, "Simulation of the urban radio propagation channel," *IEEE Trans. on Vehicul. Technol.*, vol. VT-28, pp. 213–225, Aug. 1979.

[14] D. C. Cox, "Delay doppler characteristics of multipath propagation at 910 MHz in a suburban mobile radio environment," *IEEE Trans. Antennas Propagat.*, vol. AP-20, pp. 625–635, Sept. 1972.

[15] D. C. Cox, "Time- and frequency-domain characterizations of multipath propagation at 910 MHz in a suburban mobile-radio environment," *Radio Science*, pp. 1069–1077, Dec. 1972.

[16] D. C. Cox, "910 MHz urban mobile radio propagation: Multipath characteristics in New York city," *IEEE Trans. Commun.*, vol. COM-21, pp. 1188–1194, Nov. 1973.

[17] D. C. Cox and R. P. Leck, "Distributions of multipath delay spread and average excess delay for 910-MHz urban mobile radio paths," *IEEE Trans. Antennas Propagat.*, vol. AP-23, pp. 206–213, Mar. 1975.

[18] D. L. Nielson, "Microwave propagation measurements for mobile digital radio application," *IEEE Trans. on Vehicul. Technol.*, vol. VT-28, pp. 117–132, Aug. 1978.

[19] P. J. Bickel and K. Doksum, *Mathematical Statistics: Basic Ideas and Selected Topics*. Oakland, California: Holden-Day, Inc., first ed., 1995.

Ultra-Wide Bandwidth Signal Propagation for Indoor Wireless Communications

Moe Z. Win and Robert A. Scholtz
Communication Sciences Institute
Department of Electrical Engineering-Systems
University of Southern California, Los Angeles, CA 90089-2565 USA

Mark A. Barnes
Time Domain Systems, Inc.
6700 Odyssey Drive, Suite 100, Huntsville, AL 35806 USA

Abstract— **An ultra-wide bandwidth (UWB) signal propagation experiment is performed in a typical modern office building in order to characterize the UWB signal propagation channel. The bandwidth of the signal used in this experiment is in excess of one GHz. Robustness of the UWB signal to fades is quantified through histograms and cumulative distributions of the signal quality in various locations of the building. The results show that UWB signal does not suffer fades.**

I. Introduction

PROPAGATION environments place fundamental limitations on the performance of wireless communications systems. The existence of multiple propagation paths (multipath), with different time delays, gives rise to complex, time-varying transmission channels. A line-of-site path between the transmitter and receiver seldom exists in indoor environments, because of natural or man-made blocking, and one must rely on the signal arriving via multipath.

Many propagation measurements have been made over the years on both indoor and outdoor channels with much "narrower bandwidths" [1]–[18]. A comprehensive reference on the indoor propagation channels (a total of 281 references) can be found in the tutorial survey paper by Hashemi [9]. Some of the work by Rappaport [1]–[5] and a few other papers [6]–[8] are listed here as selected references. Although the research described in this paper does not cover outdoor propagation channels, the classic works on outdoor propagation channels by Turin [10], [11], by Cox [14]-[17], and by Nielson [18] are noted here for their excellent measurement procedures and data reduction techniques. However, these measurements are inadequate for ultra-wide bandwidth (UWB) transmission systems, and characterization of UWB signal propagation channels has not been available previously in the literature. Careful characterization the UWB signal propagation channel is prudent for determining optimum methods, in order to achieve the quality communication.

The research described in this paper was supported in part by the Joint Services Electronics Program under contract F49620-94-0022, and in part by the Integrated Media Systems Center, a National Science Foundation Engineering Research Center with additional support from the Annenberg Center for Communication at the University of Southern California and the California Trade and Commerce Agency.

The corresponding author can be reached by E-mail at win@milly.usc.edu

II. Experimental Design and Measurement Apparatus

A short duration pulse, with sub-nanosecond duration, is used to probe the propagation channel. The received signal represents the convolution between the excitation pulse and the impulse response of the channel. The time varying characteristic of the channel can be observed by periodic repetition of the pulse transmission. The duration of the single pulse, inversely proportional to the bandwidth of the transmission, determines the *multipath resolution*, i.e., the minimum discernible path between individual multipath components. The period of the periodic pulse signal transmission determines the maximum measurable multipath delay. Hence, successive multipath components with differential delay greater than the width of the pulse and within one period of the periodic pulse transmission can be measured unambiguously.

A block diagram of the measurement apparatus is shown in Fig. 2. The transmitter consists of a periodic pulse generator that transmits pulses every 500 nanoseconds using a step recovery diode-based pulser connected to a UWB antenna. The receiver consists of a receiving antenna, a trigger probing antenna, a wideband low noise amplifier (LNA), and a digital sampling oscilloscope (DSO). Multipath profiles are captured by the DSO and sent over a HPIB bus to a personal computer for storage. A probe antenna, in proximity to the transmitting antenna, supplies a trigger signal to the DSO by a long fixed length coaxial cable. Therefore, all recorded multipath profiles have the same absolute delay reference, and time delay measurements of the signals arriving to the receiving antenna via different propagation paths can be made. During each of the multipath profile measurement, both the transmitter and receiver were kept stationary. The multipath propagation channel was frozen during the measurement time by ensuring that people in the vicinity of the transmitting and receiving antenna were not moving.

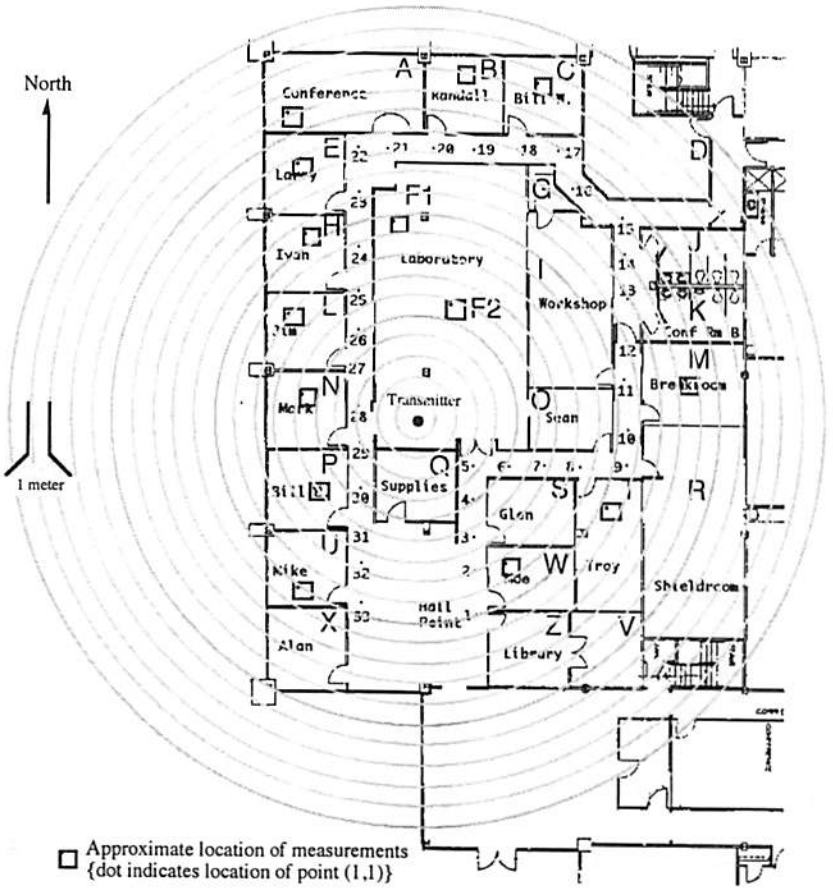

Fig. 1. The floor plan of a typical modern office building where the propagation measurement experiment was performed. The concentric circles are centered on the transmitting antenna and are a spaced at 1 meter intervals.

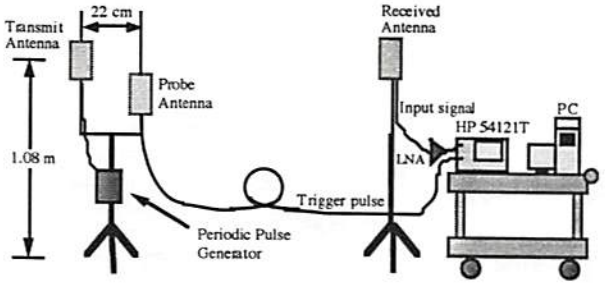

Fig. 2. A block diagram of the measurement apparatus.

III. Results

Figure 1 shows the floor plan of the modern office building where the propagation measurement experiment was performed. Each of the rooms is labeled alphanumerically. Walls around offices are framed with metal studs and covered with plaster board. The wall around the laboratory is made from acoustically silenced heavy cement block. There are steel core support pillars throughout the building, notably along the outside wall and two within the laboratory itself. The shield room's walls and door are metallic. The transmitter is kept stationary in the central location of the building near a computer server in a laboratory denoted by F. The transmitting antenna is located 165 cm from the floor and 105 cm from the ceiling. Figure 3 shows the transmitted pulses measured by the receiving antenna, located 1 m away from the transmitting antenna with the same height. Measurements were made while the vertically polarized receiving antenna was rotated about its axis in 45° steps. Measurements shown in Fig. 3 are labeled 0°, 45°, and 90°, where 0° refers to the case where the transmitting and receiving antennas are facing each other. Figure 3 illustrates that the radiation pattern of the antenna used in the experiment is circularly symmetric around the vertical axis. Notice from the building layout diagram given in Fig. 1 that the closest object to the measurement apparatus is the south wall of laboratory F, which is at least 1 meter away. The signal arriving to the receiving antenna, except the line-of-sight (LOS) signal, must travel a minimum distance of 3 meters. The initial multipaths come form floor and ceiling, 5.2 nanoseconds and 4.1 nanoseconds after the LOS signal respectively, and hence the first 10 nanoseconds of the recorded waveforms in Fig. 3 represent clean pulse arriving via the direct LOS path and not corrupted by multipath components.

Multipath profiles were measured at various locations in the rooms and hallways throughout the building. Specifically, data was collected at 14 different rooms and hallways. In each room, 300 nanoseconds wide windows of multipath measurements were made at 49 different locations over a 3

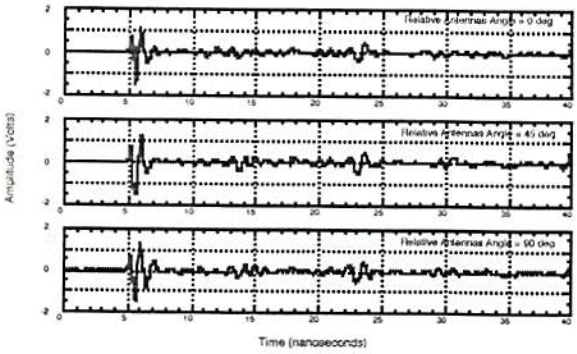

Fig. 3. Transmitted pulses measured by the receiving antenna located 1 m away from the transmitting antenna with the same height. Measurements were made while the vertically polarized receiving antenna was rotated about its axis, where 0° refers to the case in which the transmitting and the receiving antenna are facing at each other.

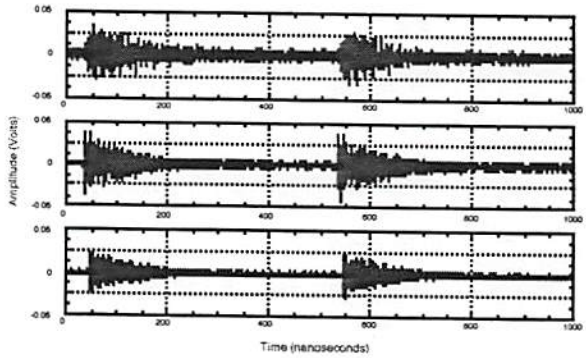

Fig. 4. Average multipath measurements of 32 sequentially measured multipath profiles where the receiver is located at the same exact locations in offices U, W and M. The measurement grids are 10, 8.5, and 13.5 meters away from the transmitter respectively.

feet by 3 feet grid. The approximate location of these measurement grids in each room are shown in Fig. 1. They are arranged spatially in a 7x7 square grid with 6 inch spacing. Each location on the grid is numbered as (i, j), where i represents the rows and j represents the column of the grid. As a convention, the top row is always parallel and adjacent to the north wall of the room. The receiving antenna is located 120 cm from the floor and 150 cm from the ceiling. This antenna height is envisioned to be typical for future indoor applications.

A single multipath profile of 1000 nanoseconds long, which captures the response of two successive probing pulses, was also made in each room. Figure 4 shows the 1000 nanoseconds long measurement, where two back to back multipath measurement cycles are captured by the receiver located in offices U, W and M respectively. The approximate distances between the transmitter and the location of these measurement grids located in offices U, W and M are 10, 8.5, and 13.5 meters respectively. Figure 4 also shows that the response of the first probing pulse has decayed (is sufficiently settled down) before the next pulse arrives at the antenna. Substantial differences in the noise floor at various locations throughout the building is observed. Specifically, the multipath profiles recorded in the offices W and M have a substantially lower noise floor compared to the profiles recorded in office U. This can be explained, with the help of the floor plan given in Fig. 1, by observing: Office U is situated at the edge of the building with large glass window. Offices W and M are situated roughly in the middle of the building. Furthermore, offices W and M are adjacent to room R which is shielded from electromagnetic radiation. Interference from radio stations, television stations, cellular and paging towers, and other external electromagnetic interference (EMI) sources are attenuated by the shielded walls and multiple layers of other regular walls. The increased noise floor is generally observed for all the measurements made in offices located at edges of the building with large glass windows.

Figure 5 shows the averaged multipath profiles measured in office P at locations (4,1), (4,4) and (4,7) along the horizontal cross section of the grid with three different aligned positions of one foot apart. The distance between the receiver in the office P and the transmitter is approximately 6 meters, relatively close compared to other rooms. The data that is collected in this room represents typical UWB signal transmissions for the "high SNR" case. Notice that the direct path response (leading edge of the responses) suggests that the location of the receiver for the lower trace is closer to the transmitter than that of the upper trace. This fact can be verified easily by the floor plan given in Fig. 1. Multipath delay spreads on the order of a hundred nanoseconds were observed.

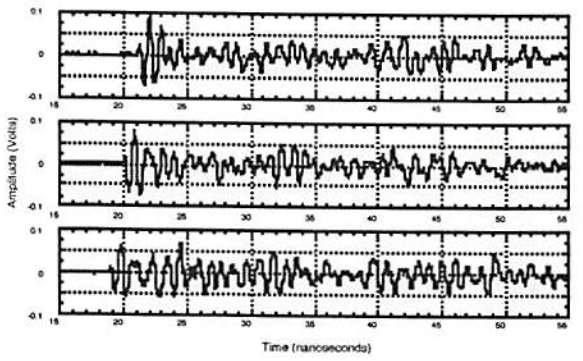

Fig. 5. Averaged multipath profiles of 40 nanoseconds window measured in office P, along the horizontal cross section of the grid at three different aligned positions of one foot apart. The transmitter is approximately 6 meters from the receiver representing typical UWB signal transmissions for the "high SNR" case.

To understand the effect of office doors, two multipath profiles were recorded at the same location in office B. One profile was recorded with the office door open and the other profile was recorded with the office door closed. No noticeable difference between these two measurements was observed. The effect of the large computer monitor was also considered. The receiving antenna was placed near a

large computer monitor in office C and measurements were made. A slight increase in noise floor was observed when the computer monitor was turned on.

IV. Robustness of the UWB Signal to Fades

Robustness of the UWB signal to fades can be assessed by measuring the received energy in various locations of the building relative to the received energy at a reference point. Mathematically, the *signal quality* at a location (i, j) can be defined as

$$Q_{i,j} = 10\log_{10} E_{i,j} - 10\log_{10} E_{\text{ref}} \quad [\text{dB}]. \qquad (1)$$

The received energy $E_{i,j}$ at a location (i, j) is given by

$$E_{i,j} = \int_0^T |r_{i,j}(t)|^2 dt, \qquad (2)$$

where $r_{i,j}(t)$ is the measured multipath at location (i, j) and T is the observation time. The reference energy E_{ref} is chosen to be the energy in the LOS path measured by the receiver located 1 meter away from the transmitter.

The signal quality $Q_{i,j}$ is calculated for the measurements made at 741 different locations (14 different rooms with 49 locations/room, 21 locations in the shield room, and 34 locations around the hallways). First and second order local statistics of the signal quality are calculated. That is, the mean and variance of the signal quality based on 49 spatial sample points (except 21 spatial points for room R, and 34 spatial points for hallways) in each room are estimated by

$$\hat{\mu} = \frac{1}{N}\sum_{i,j} Q_{i,j}\,, \qquad (3)$$

and

$$\hat{\sigma}^2 = \frac{1}{N-1}\sum_{i,j}(Q_{i,j} - \hat{\mu})^2\,. \qquad (4)$$

It can be shown that these estimate are a function of complete sufficient statistics if the received signal energy $E_{i,j}$ are random samples from normal families. Then by the Lehmann-Scheffé theorem [19], the estimates given by (3) and (4) are unique and gives the uniformly minimum variance unbiased estimates.

Table I shows the estimates of the mean and the variance of the signal quality in each room based on 49 sample (except 21 samples for room R, and 34 samples for hallways). The histograms and the cumulative distribution functions of the signal quality based on 49 spatial local sample points in each room (except 21 samples for room R, and 34 samples for hallways) are shown in Fig. 6 and Fig. 7 respectively. These figures along with Table I indicates that the signal energy per received multipath waveform varies by at most 5 dB as receiving position varies over the measurement grid within a room. This clearly demonstrates the robustness of UWB signal transmissions in a severe fading environments, and that UWB radio have the potential for fade-free communications even in this severe indoor multipath environment. In some situations, the transmitted power potentially can be reduced by 10-30 dB, since only a *small fading margin* in communication link budget is required to guarantee the reliable communication of an UWB radio.

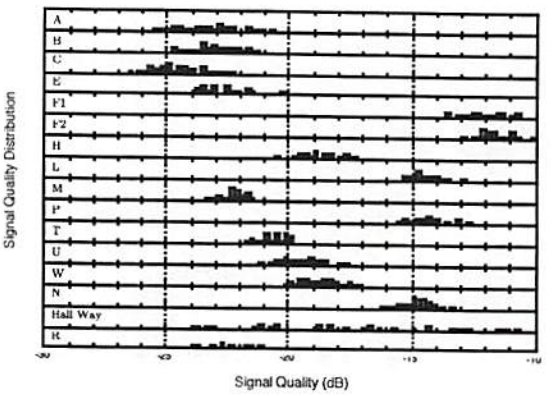

Fig. 6. The histograms of the signal quality based on 49 spatial sample points (except 21 spatial points for room R, and 34 spatial points for hallways) in each room. Total of 741 measurements were used in this plot.

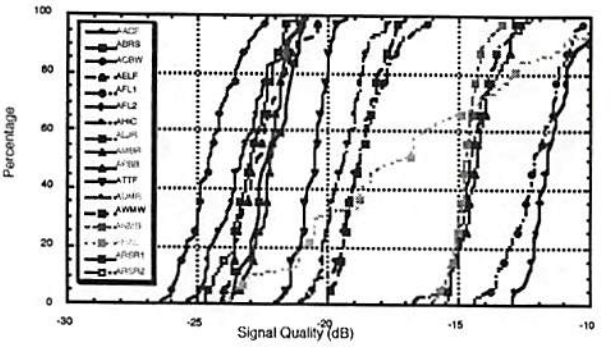

Fig. 7. The cumulative distribution functions of the signal quality based on 49 spatial sample points (except 21 spatial points for room R, and 34 spatial points for hallways) in each room. Total of 741 measurements were used in this plot.

V. Conclusions

Extensive UWB propagation measurements were made in 14 different rooms and hallways of a modern office building using a periodic pulse generator that transmits UWB pulses every 500 nanoseconds. Multipath measurements of 300 nanoseconds long window were made at 49 different locations arranged spatially in a 7x7 square grid with 6 inch spacing covering 3 feet by 3 feet. The same absolute delay reference for all recorded multipath profiles was achieved, and the time delay measurements of the signals arriving to the receiving antenna via different propagation paths were made.

Increased noise floor was generally observed for all the measurements made in offices located at edges of the building with large glass windows; and is attributed to radio sta-

TABLE I
SIGNAL QUALITY STATISTICS

Office	$\approx$ distance (meters)	Minimum (dB)	Maximum (dB)	$\hat{\mu}$ (dB)	Median (dB)	$\hat{\sigma}$ (dB)	# of Samples
F2	5.5	-12.9970	-9.64586	-11.5241	-11.6813	0.8161	49
N	5.5	-16.0060	-13.2949	-14.7260	-14.7690	0.5892	49
P	6.0	-15.5253	-12.2185	-14.2373	-14.2820	0.8091	49
L	8.0	-16.6966	-12.4310	-14.4500	-14.5538	0.8342	49
W	8.5	-20.0157	-17.0351	-18.7358	-18.7425	0.7622	49
F1	9.5	-14.4064	-9.79770	-12.0986	-12.1407	1.0563	49
H	10.0	-21.0415	-16.1628	-18.7141	-18.8142	1.1240	49
U	10.0	-21.1719	-17.6232	-19.4275	-19.4092	0.8024	49
T	10.5	-21.9113	-19.2986	-20.6100	-20.5419	0.5960	49
R	10.5	-23.7221	-20.8867	-22.2675	-22.3851	0.8686	21
M	13.5	-23.8258	-20.9277	-22.2568	-22.2064	0.6439	49
E	13.5	-24.1454	-20.2000	-22.5973	-22.7824	1.0332	49
A	16.0	-25.4171	-20.7822	-23.2826	-23.3541	1.1512	49
B	17.0	-24.7191	-21.2006	-22.9837	-22.9987	0.8860	49
C	17.5	-26.4448	-22.3120	-24.4842	-24.5777	1.0028	49
Hallways		-23.8342	-6.72469	-16.9317	-17.3286	4.5289	34

tions, television stations, cellular and paging towers, and other external electromagnetic interference (EMI) sources coexisting in the same bandwidth. The effects of office doors, large computer monitors were investigated and no substantial effects were observed. Robustness of the UWB signal to fades is quantified through histograms and cumulative distributions of the signal quality in various locations of the building. The results show that UWB signal does not suffer fades. Therefore, very little fading margin is required to guarantee the reliable communication.

ACKNOWLEDGMENTS

The authors wish to thank Troy Fuqua, Glenn Wolenec, Ivan Cowie, and Larry Fullerton of Time Domain Systems, and Paul Withington of Pulson Communications for several helpful discussions concerning the technology, capabilities, and signal processing of impulse signals.

REFERENCES

[1] J. B. Andersen, T. S. Rappaport, and S. Yoshida, "Propagation measurements and models for wireless communications channels," *IEEE Commun. Mag.*, vol. 33, pp. 42–49, Jan. 1995.

[2] T. S. Rappaport and C. D. McGillem, "UHF fading in factories," *IEEE J. Select. Areas Commun.*, vol. SAC-7, pp. 40–48, Jan. 1989.

[3] T. S. Rappaport, "Characterization of UHF multipath radio channels in factory buildings," *IEEE Trans. Antennas Propagat.*, vol. AP-37, pp. 1058–1069, Aug. 1989.

[4] T. S. Rappaport, S. Y. Seidel, and K. Takamizawa, "Statistical channel impulse response models for factory an open plan building radio communication system design," *IEEE Trans. Commun.*, vol. COM-39, pp. 794–807, May 1991.

[5] S. Y. Seidel and T. S. Rappaport, "914 MHz path loss prediction models for indoor wireless communications in multifloored buildings," *IEEE Trans. Antennas Propagat.*, vol. AP-40, pp. 207–217, Feb. 1992.

[6] D. M. J. Devasirvatham, "Multipath time delay jitter measured at 850 MHz in the portable radio environment," *IEEE J. Select. Areas Commun.*, vol. SAC-5, pp. 855–861, June 1987.

[7] A. A. Saleh and R. A. Valenzuela, "A statistical model for indoor multipath propagation," *IEEE J. Select. Areas Commun.*, vol. SAC-5, pp. 128–137, Feb. 1987.

[8] R. J. Bultitude, S. A. Mahmoud, and W. A. Sullivan, "A comparison of indoor radio propagation characteristics at 910 MHz and 1.75 GHz," *IEEE J. Select. Areas Commun.*, vol. SAC-7, pp. 20–30, Jan. 1989.

[9] H. Hashemi, "The indoor radio propagation channel," *Proc. IEEE*, vol. 81, pp. 943–968, July 1993.

[10] G. Turin, F. D. Clapp, T. L. Johnston, S. B. Fine, and D. Lavry, "A statistical model of urban multipath propagation," *IEEE Trans. on Vehicul. Technol.*, vol. VT-21, pp. 1–9, Feb. 1972.

[11] G. Turin, "Introduction to spread-spectrum antimultipath techniques and their application to urban digital radio," *Proc. IEEE*, vol. 68, pp. 328–353, Mar. 1980.

[12] H. Suzuki, "A statistical model for urban radio propagation," *IEEE Trans. Commun.*, vol. 25, pp. 673–680, July 1977.

[13] H. Hashemi, "Simulation of the urban radio propagation channel," *IEEE Trans. on Vehicul. Technol.*, vol. VT-28, pp. 213–225, Aug. 1979.

[14] D. C. Cox, "Delay doppler characteristics of multipath propagation at 910 MHz in a suburban mobile radio environment," *IEEE Trans. Antennas Propagat.*, vol. AP-20, pp. 625–635, Sept. 1972.

[15] D. C. Cox, "Time- and frequency-domain characterizations of multipath propagation at 910 MHz in a suburban mobile-radio environment," *Radio Science*, pp. 1069–1077, Dec. 1972.

[16] D. C. Cox, "910 MHz urban mobile radio propagation: Multipath characteristics in New York city," *IEEE Trans. Commun.*, vol. COM-21, pp. 1188–1194, Nov. 1973.

[17] D. C. Cox and R. P. Leck, "Distributions of multipath delay spread and average excess delay for 910-MHz urban mobile radio paths," *IEEE Trans. Antennas Propagat.*, vol. AP-23, pp. 206–213, Mar. 1975.

[18] D. L. Nielson, "Microwave propagation measurements for mobile digital radio application," *IEEE Trans. on Vehicul. Technol.*, vol. VT-28, pp. 117–132, Aug. 1978.

[19] P. J. Bickel and K. Doksum, *Mathematical Statistics: Basic Ideas and Selected Topics*. Oakland, California: Holden-Day, Inc., first ed., 1995.